LAGRANGIAN TRAJECTORIES AND SETTLING VELOCITY OF SNOWFLAKES: OBSERVATION OF PARTICLE-TURBULENCE DYNAMICS

Andras Nemes
Dept. of Aerospace Engineering & Mechanics
Univerisity of Minnesota
Minneapolis, MN 55455, USA
nemesa@umn.edu

Teja Dasari
Dept. of Mechanical Engineering
University of Minnesota
Minneapolis, MN 55455, USA
dasar009@umn.edu

Michele Guala
Dept. of Civil Engineering
University of Minnesota
Minneapolis, MN 55455, USA
mguala@umn.edu

Jiarong Hong
Dept. of Mechanical Engineering
University of Minnesota
Minneapolis, MN 55455, USA
jhong@umn.edu

Filippo Coletti
Dept. of Aerospace Engineering & Mechanics
University of Minnesota
Minneapolis, MN 55455, USA
fcoletti@umn.edu

ABSTRACT

We report on optical field measurements of snow settling in atmospheric turbulence at Re_λ = 940. It is found that the snowflakes exhibit hallmark features of inertial particles in turbulence. The snow motion is analyzed in by large-scale particle imaging, while sonic anemometry is used to characterize the flow field. Additionally, the snowflake size and morphology are assessed by digital in-line holography. The low volume fraction and mass loading imply a one-way interaction with the turbulent air. Acceleration probability density functions show wide exponential tails consistent with laboratory and numerical studies of homogeneous isotropic turbulence. Invoking the assumption that the particle acceleration has a stronger dependence on the Stokes number than on the specific features of the turbulence (e.g. precise Reynolds number and large-scale anisotropy), we make inferences on the snowflakes' aerodynamic response time. In particular, we observe that their acceleration distribution is consistent with that of particles of Stokes number in the range 0.1–0.4 based on the Kolmogorov time scale. The still-air terminal velocities estimated for the resulting range of aerodynamic response times are significantly smaller than the measured snow particle fall speed. This is interpreted as a manifestation of settling enhancement by turbulence, which is observed here for the first time in a natural setting.

INTRODUCTION

In gaseous flows, such as atmospheric flows, even microscopic solid particulates and liquid droplets have significant inertia due to their density being much greater than the surrounding fluid. Indeed, much of the research on inertial particles in turbulence has been motivated by the need to understand and predict atmospheric phenomena. Examples range from sand storms and the physics of aeolian transport, to the formation and precipitation of atmospheric clouds. The latter area in particular has been the subject of great focus due to its importance in climate prediction models. Aided by increasing computational power, numerical simulations have significantly contributed to our understanding of the impact of turbulence on the condensational and collisional growth of clouds and its influence across the vast range of scales at play. Computational representations are, however, necessarily simplified. Even when all pertinent flow scales are resolved through direct numerical simulation (DNS), stringent assumptions are needed to calculate the motion of the realistically large number of particles. The most common simplification is the use of the point-particle approximation, e.g. the modeling of each particle as a point mass of zero volumem, which can either be passively advected by the flow or exchange momentum and potentially modify the turbulence (Squires & Eaton 1990, 1991; Elghobashi & Truesdell 1993). Experimental studies have investigated canonical flows (often approximating homogeneous isotropic turbulence) interacting with spherical microscopic particles or droplets (Aliseda et al. 2002, Wood, Hwang & Eaton 2005, Ayyalasomayajula et al. 2006, Monchaux, Bourgoin & Cartellier 2010, Good et al. 2014) and have qualitatively confirmed many of the findings from numerical simulations. However, Reynolds numbers relevant to environmental phenomena cannot presently be achieved by DNS, and are in general hard to obtain even in laboratory experiments, unless special measures are taken to reduce the fluid viscosity (Bodenschatz et al. 2014).

In this scenario, field experiments demonstrating the role of particle-turbulence dynamics in natural phenomena are necessary for understanding of the flow physics in realistic conditions, and represent a key step towards the implementation of results from fundamental fluid mechanics studies into weather forecasting models. Indeed the single-phase turbulence dynamics in the atmospheric surface layer (i.e. the inner part of the planetary boundary layer where the velocity profile follows the logarithmic law) have been the subject of several in situ campaigns that have contributed to reconcile results from laboratory and atmospheric flows at

disparate Reynolds numbers (Hutchins et al. 2012). Field measurements focused on particle-turbulence interaction in the atmosphere are comparatively scarce. This is likely due to the massive range of scales involved, from the particle size to the energy-containing eddies, and consequently the daunting level of resolution and dynamic range needed. Notable recent examples include: Ditas et al. (2012), who characterized the turbulence and droplet size distribution within stratocumulus clouds using an observation system suspended from a helicopter; Beals et al. (2015), who deployed an airborne holography system to show sharp inhomogeneities in the cloud droplet distribution down to the centimeter scale; and Siebert et al. (2015), who carried out high-resolution measurements of cloud droplet size distribution and number density in a mountaintop field station.

In the present paper we report on the first field study in which Lagrangian trajectories and settling velocity of snowflakes are directly observed in the atmospheric surface layer. We use a large-scale imaging procedure recently employed to characterize the wake of a full scale wind turbine (Hong et al. 2014) and the profile of the atmospheric surface layer (Toloui et al. 2014). We simultaneously characterize the air turbulence using sonic anemometry and the hydrometeor morphology using digital in-line holography. We find that snowflake exhibit hallmark features of inertial particles in homogeneous turbulence.

EXPERIMENTAL METHODOLOGY

The field deployment to acquire the present data took place at the University of Minnesota Eolos Wind Energy Research Field Station (Rosemount, MN). The topography in the 2 km around the measurement location is nearly flat, with a few very sparse 1–2 story buildings located several hundred meters away. A measurement tower at the site comprises four three-dimensional sonic anemometers (20 Hz sampling rate, heights z = 10, 30, 80, and 129 m, CSAT3, Campbell Scientific), and six cup-and-vane anemometers (1 Hz sampling rate, heights z = 7, 27, 52, 77, 102, and 126 m), each one mounted on a 5 m long boom equipped with additional temperature and relative humidity sensors. Further details on the site and meteorological tower instruments are given in Hong et al. (2014) and Toloui et al. (2014).

Digital in-line holography is employed to determine the morphology and size distribution of snowflakes during the deployment. The system consists of a diode laser, a beam expander, and a collimating lens to produce a 50 mm diameter beam. The entire setup is sealed inside a 6 cm x 6 cm acrylic container, with an opening at the top allowing snowflakes to fall through. The laser light scattered by the snowflakes interferes with the non-scattered portion of the laser beam to form a hologram, captured on a CMOS camera at resolution of 16 μm/pixel. Snowflake images are obtained through numerical reconstruction and segmentation of the recorded holograms at different distances away from the recording plane. 138 snowflakes were captured over a duration of 64 minutes. Sample images are reported in Fig. 1.

For illuminating the snowflakes we used a 5 kW searchlight aimed at a curved reflector to generate a lightsheet 0.3 m in thickness and approximately aligned with the wind direction. A CMOS camera was operated at 120 Hz for 720 x 1080 pixels and located at a stand-off distance of 25 m from the lightsheet. Tilting the optical axis 21° from the horizontal, the camera imaged a field of view of 7 m x 4 m (Fig. 2). We present results acquired over a 5 minute window. Eulerian velocity fields were computed using particle image velocimetry (PIV) with an iterative adaptive correlation scheme, a final pass of 32 x 32 pixels, and 50% overlap. At a 5.46 mm/pixel ratio, the vector spacing was 87 mm, which compares to a Kolmogorov length scale of 1.3 mm. Particle tracking velocimetry (PTV) provided Lagrangian particle trajectories extracted using the four-frame best estimate algorithm proposed by Ouellette et al. (2006). The initial vector estimate was based on interpolated vectors from the final pass of PIV to reduce the particle neighborhood search to a 3 pixel radius. The tracking algorithm was applied to particle centroids located using Gaussian 3 point fitting to 16-bit band-passed grayscale images around peaks passing a strict maxima criterion on particle intensity, so as to minimize peak-locked statistics. Figure 3 shows a snapshot with a close-up view of snowflake images and their centroid. The sampling period of 1/120 s was over 15 times smaller than the Kolmogorov time scale.

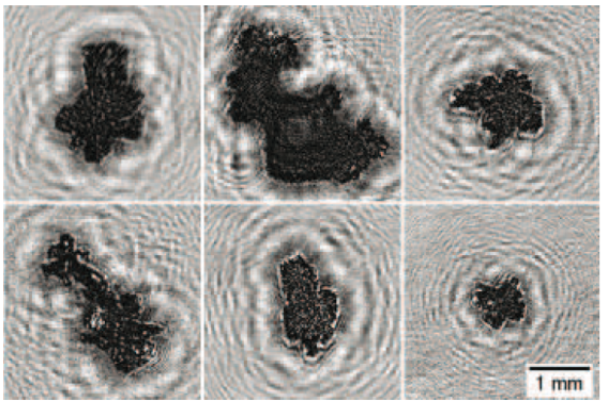

Fig. 1. Samples of snowflake images after holographic reconstruction.

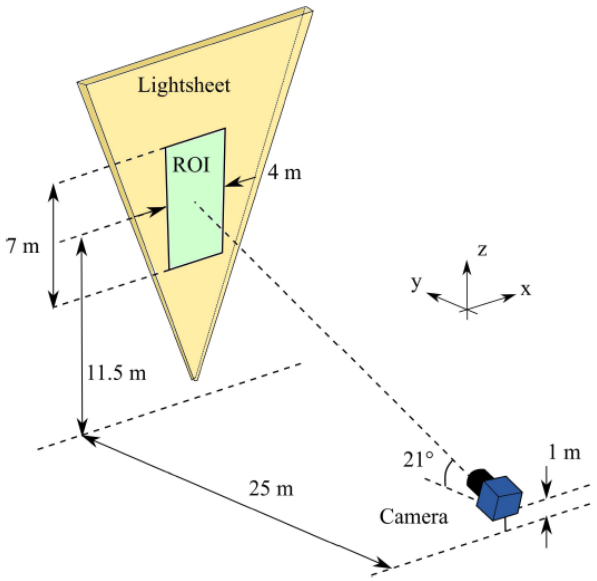

Figure 2. Schematic of the field deployment for large-scale imaging of snow particles.

RESULTS

The sonic anemometer at z = 10 m was used to provide statistics of the atmospheric turbulence. Records of the velocity and temperature from the meteorological tower are plotted in Fig. 4. We use Taylor hypothesis based on a convection velocity equal to the local mean wind velocity to convert temporal into spatial statistics. The integral length scale is calculated from the temporal autocorrelation of the sonic anemometry, aslo shown in Fig. 4. The integral length scale calculated from the velocity autocorrelation is L = 4.9 m, the rms velocity fluctuation is u' = 0.16 m/s, and the turbulent dissipation is approximated as $\varepsilon = u'^3/L$, leading to Kolmogorov scales η = 1.26 mm and τ_η = 0.13 s, and a Taylor microscale Reynolds number Re_λ = 940.

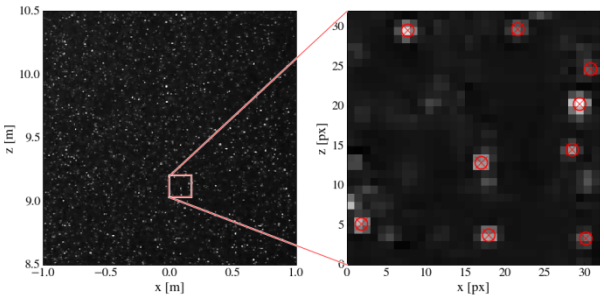

Figure 3. Sample acquisition of snow particles zoomed in on (a) a 2 m x 2m m field of view, (b) a 32 x 32 pixel subset of the image showing individual snow particles and their centroid locations.

Figure 5 shows the hydrometer equivalent diameter distribution. The mean diameter of the snowflakes measured from holography was D_p = 1.09 mm with a standard deviation of 0.45 mm. The images showed fairly compact hydrometeor shapes, with a major-to-minor axis aspect ratio of 1.39. The observed hydrometeors fall between the categories of graupel (resulting from the inverse sublimation of supercooled water on an ice core) and heavily rimed crystals (Pruppacher & Klett 1997).

Using PIV we measure a mean horizontal snow particle velocity of U_p = 1.24 m/s and a mean vertical (settling) velocity of W_p = 0.86 m/s, both quantities being fairly homogeneous within the field of view. The horizontal velocity is close to the wind speed projected into the imaging plane, and therefore the fall speed is taken as the mean slip velocity, leading to a snow particle Reynolds number $Re_p = W_p D_p/\nu = 70$.

A hallmark feature of inertial particles in turbulence is that their Lagrangian acceleration statistics differ from those of fluid tracers (Toschi & Bodenschatz 2009), and the moments of the acceleration PDF are sensitive to the particle Stokes number (Bec et al. 2006, Salazar and Collins 2012). Being related to small-scale features of the flow, the dependence of the acceleration with St is not expected to be strongly influenced by the specific type of turbulent flow, at least at high Reynolds numbers. For example, the acceleration PDF obtained by Gerashchenko et al. (2008) for inertial particles in the outer region of a turbulent boundary layer closely matched those obtained in active grid turbulence by Ayalasomayyajula et al (2006). We leverage these behaviors to estimate the Stokes number of the snowflakes.

We calculate snow particle acceleration following the approach described by Voth et al. (2002) and modified by Mordant, Crawford & Bodenschatz (2004). A total of about 87000 snow particle trajectories exceeding 32 frames were used to calculate acceleration statistics by convolving them with the normalized second derivative of a Gaussian kernel.

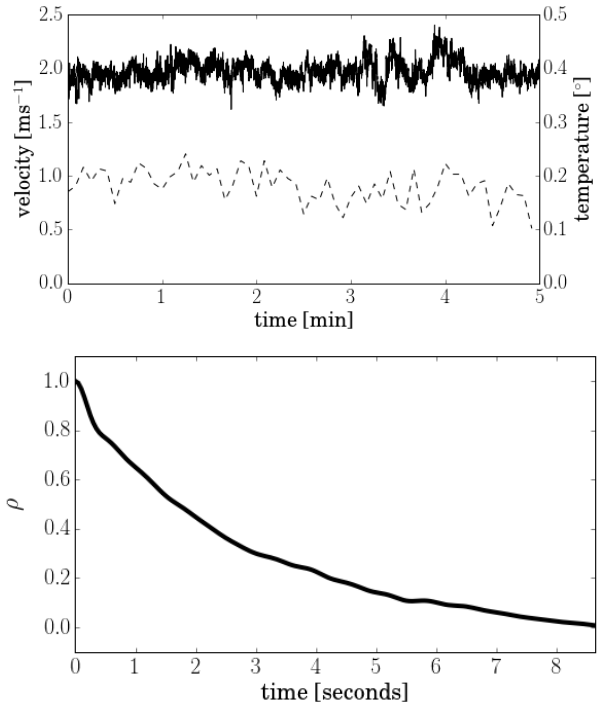

Figure 4. Top: 5 minute window of the sonic anemometer data showing wind velocity and air temperature. Bottom: Auto-correlation of 5 min window in top panel used to calculate the integral time and length scale.

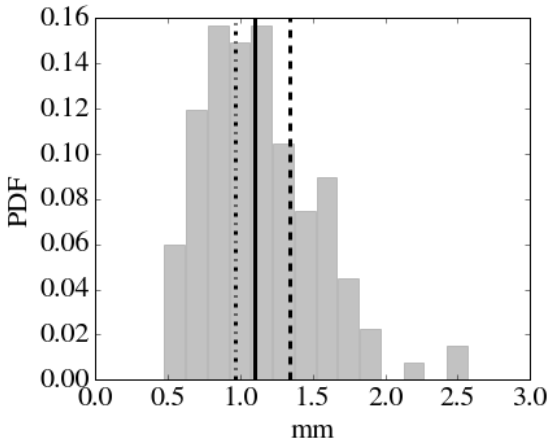

Figure 5. Histogram of equivalent diameter of snowflakes obtained from DIH measurements during the deployment. The solid line denotes the mean equivalent diameter based on area, the dashed line denotes the mean diameter based on the major axis, and the dash-dotted line denotes the mean diameter based on the minor-axis.

Figure 6 shows a sample of the reconstructed trajectories. The convolution of the derivative of the Gaussian kernel acts both as a numerical derivative and a low-pass filter of the raw data. This is required to reduce the noise associated with particle position uncertainty and to prevent it from contaminating the Lagrangian statistics. The kernel needs to be

applied over an appropriate number of consecutive frames, i.e. an appropriate convolution time interval τ_g. For too short intervals particle position uncertainty contaminates the statistics; for too long intervals strong acceleration events are damped by excessive filtering. Following the above-mentioned studies, we chose the smallest τ_g for which the acceleration variance retains an exponential dependency on the interval width. This corresponds to 29 frames and is of order τ_η (Voth et al. 2002, Gerashchenko et al. 2008). We measure an rms acceleration $a' = 0.505$ ms^{-2} and a kurtosis $K = \langle a^4 \rangle / a'^4 = 5.23$.

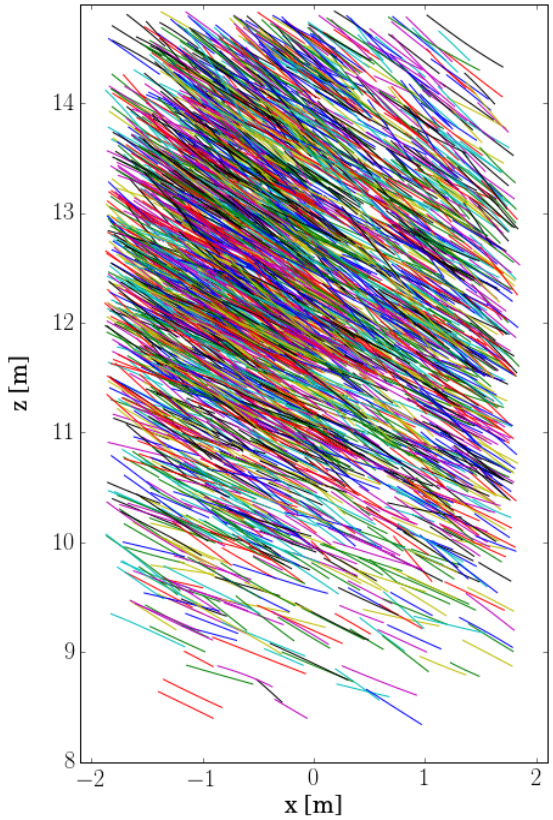

Fig. 6. The 600 longest trajectories reconstructed by PTV.

We then use the acceleration distribution normalized by a' (Fig. 7) to infer the snowflake Stokes number $St = \tau_p/\tau_\eta$. The acceleration PDF shows stretched exponential tails typical of Lagrangian particles in turbulence. Data from previous experimental and numerical studies are also shown. Although there is scatter in the experimental data, the acceleration PDF we measure falls in the range spanned by the St = 0.09 case of Ayyalasomayajula et al. (2006) and the St = 0.37 case of Bec et al. (2006). Therefore we infer for the snowflakes a Stokes number in the range St = 0.09 - 0.37. Accounting for the differences between our atmospheric flow and those in previous studies, one may expect differences in the acceleration PDF, notably due to turbulence Reynolds number. However, the results of Voth et al. (2002) indicate that the acceleration kurtosis of fluid tracers reaches a plateau for above $Re_\lambda = 500$, and for inertial particles in turbulence the recent DNS of Ireland et al. (2016) shows only small changes of the kurtosis of particle accelerations above $Re_\lambda = 398$.

From the particle Stokes number and the Kolomogorov time scale, it follows that the aerodynamic response time of the snowflakes is in the range $\tau_p = 12$ - 48 ms. This allows us to directly evaluate the range for terminal velocity the snowflakes would have in stil air, i.e. $V_T = \tau_p g = 0.12$ - 0.47 m/s. This is several times smaller than the observed mean settling velocity, as shown in Fig. 8 which compares the still-air settling velocity range and the observed probability distribution of the snowflake vertical velocity. This is in broad agreement with some of the previous laboratory measurements (Aliseda et al. 2002), and suggests that the preferential sweeping mechanism described by Wang & Maxey (1993) is active and plays a key role in determining the fall speed of snowflakes in atmospheric turbulence.

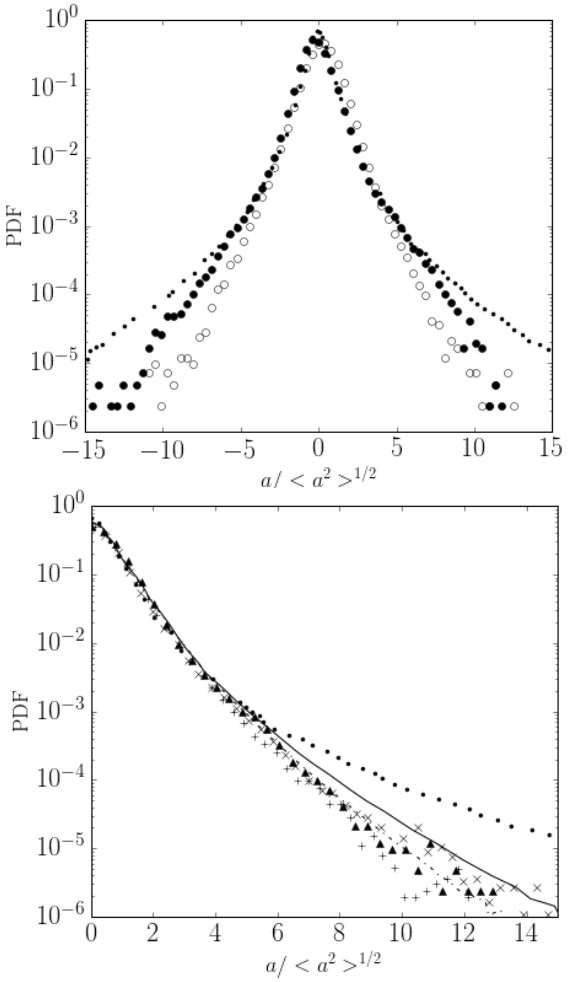

Fig. 7. Top: PDFs of horizontal (open circles) and vertical (filled circles) snowflake accelerations compared to St = 0 (Mordant et al. 2004, small filled circles). Bottom: PDF of snowflake acceleration magnitude (black triangles), compared with Mordant et al. 2004 (small filled circles), Ayyalasomayajula 2006 (St=0.09, X; St=0.15, +), and Bec et al. 2006 (St=0.16, solid line; St=0.37, dash-dotted line).

Because of the complexity of the particle-turbulence interaction, there are multiple candidates for the role of dominant velocity scale and temporal scale determining the settling enhancement. After Wang & Maxey (1993), τ_η is usually considered the appropriate time scale (hence the usual definition of the Stokes number), while both u' and u_eta have been proposed as characteristic velocity scale. Wang & Maxey

(1993) commented that the low-vorticity regions where particles accumulate resemble the large-scale flow features characterized by u', and Yang & Lei (1998) argued that u' is the velocity scale that determines the drag on the settling particles, which is a crucial element for the increase of the settling rate. Still the issue has remained open, partly because the scale separation in numerical and experimental studies has been limited, with u'/u_η at most about 7. We can use the present high Reynolds number case to gain insight on this question using the following argument. When gravity is acting, the particle-turbulence interaction is described not only by St but also by the settling parameter Sv, i.e. the ratio of the settling velocity to either the small scale velocity, $Sv_\eta = Vt/u_\eta$, or the large scale velocity, $Sv_L = Vt/u'$. Depending on whether u_eta or u' is the characteristic velocity scale for preferential sweeping, one expects maximum settling velocity enhancement when either $Sv_\eta \approx 1$ or $Sv_L \approx 1$ (which is analogous to the condition of both Stokes and Froude number $Fr = StSv^2$ being of order unity, see Davila & Hunt 2001 and Rosa et al. 2016). In our field experiment there is substantial scale separation, with $Re_\lambda \approx 1000$, $L/\eta \approx 3750$, and $u'/u_\eta \approx 16$. From the estimated range for Vt, we have $Sv_\eta = 11\text{-}47$ and $Sv_L = 0.7 - 2.9$. In other words the observed snow particles, whose fall speed is greatly increased by the turbulence, have a still-air settling velocity much larger than the Kolmogorov velocity but of the same order as the large-eddy velocity. This is consistent with the proposal that u' is indeed the appropriate velocity scale associated to turbulence-enhanced settling. One may argue that much lighter snow particles (with $Sv_\eta = O(1)$ and $Sv_L << 1$) could display even more strongly enhanced settling. This seems unlikely though, at least in the present conditions, since such particles would have $St_\eta << 1$ and therefore would be unlikely to experience preferential sweeping.

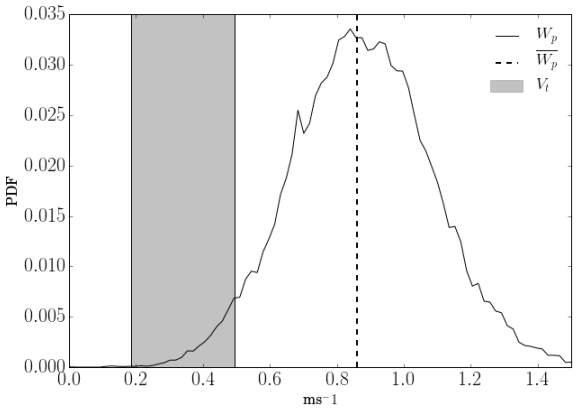

Fig. 8. Comparison of the measured distribution (solid line) and average (dashed line) of the snowflake settling velocity W_p, against the predicted range of still-air terminal velocity V_T (gray region).

CONCLUSIONS

We have presented results from direct observation of snowflake trajectories in atmospheric turbulence. We characterized the air flow, the hydrometeor properties, and their motion using a combination of meteorological tower data, digital in-line holography, and large-scale particle imaging. The hydrometeors, classified as graupels or heavily rimed crystals, were fairly compact and with sizes of the order of the Kolmogorov length. Despite the non-canonical aspects of the natural precipitation (e.g. non-sphericity and poly-dispersity of the dispersed phase and large-scale anisotropy of the environmental turbulence), the snowflakes motion exhibits signature features described by laboratory experiments and numerical simulations investigating inertial particles in turbulence. The snow particle velocity fluctuations display a Gaussian distribution, while the acceleration distribution has stretched exponential tails. By comparing with previous studies of particle acceleration in homogeneous turbulence, we deduce that the observed snowflakes have a Stokes number (based on the Kolmogorov time scale) between 0.09 and 0.37. Consistent with previous studies at much lower Reynolds numbers, the mean settling velocity is found to be much greater than the expected still-air fall speed. Because the turbulent flow was stationary during the observation window, the increase in settling velocity is deemed to be caused by the turbulent motion rather than by oscillations in wind direction. It is therefore concluded that the preferential sweeping mechanism described by Wang & Maxey (1993) is active and plays a key role in determining the fall speed of snowflakes in atmospheric turbulence. The observed particles have $Sv_\eta = O(0.1)$ and $Sv_L = O(1)$, suggesting that τ_η and u' are the dominant temporal and velocity scales in the process of settling enhancement.

Given the typical scales of atmospheric turbulence, conditions similar to the ones encountered here could be met by various types of snow and even by other classes of hydrometeors. Further field observations are warranted to investigate other forms of precipitation and different regions of the parameter space.

REFERENCES

Aliseda, A., Cartellier, A., Hainaux, F., & Lasheras, J. C. (2002). Effect of preferential concentration on the settling velocity of heavy particles in homogeneous isotropic turbulence. *Journal of Fluid Mechanics*, *468*, 77-105.

Ayyalasomayajula, S., Gylfason, A., Collins, L. R., Bodenschatz, E., & Warhaft, Z. (2006). Lagrangian measurements of inertial particle accelerations in grid generated wind tunnel turbulence. *Physical Review Letters*, *97*(14), 144507.

Beals, M. J., Fugal, J. P., Shaw, R. A., Lu, J., Spuler, S. M., & Stith, J. L. (2015). Holographic measurements of inhomogeneous cloud mixing at the centimeter scale. *Science*, *350*(6256), 87-90.

Bec, J., Biferale, L., Boffetta, G., Celani, A., Cencini, M., Lanotte, A., ... & Toschi, F. (2006). Acceleration statistics of heavy particles in turbulence.*Journal of Fluid Mechanics*, *550*, 349-358.

Bodenschatz, E., Bewley, G. P., Nobach, H., Sinhuber, M., & Xu, H. (2014). Variable density turbulence tunnel facility. *Review of Scientific Instruments*,*85*(9), 093908.

Davila, J., & Hunt, J. C. (2001). Settling of small particles near vortices and in turbulence. *Journal of Fluid Mechanics*, *440*, 117-145.

Ditas, F., Shaw, R. A., Siebert, H., Simmel, M., Wehner, B., & Wiedensohler, A. (2012). Aerosols-cloud microphysics-thermodynamics-turbulence: evaluating supersaturation in a marine stratocumulus cloud. *Atmospheric Chemistry and Physics*, *12*(5), 2459-2468.

Elghobashi, S., & Truesdell, G. C. (1993). On the two-way interaction between homogeneous turbulence and dispersed

solid particles. I: Turbulence modification. Physics of Fluids A: Fluid Dynamics (1989-1993), 5(7), 1790-1801.

Garrett, T. J., & Yuter, S. E. (2014). Observed influence of riming, temperature, and turbulence on the fallspeed of solid precipitation. *Geophysical Research Letters*, *41*(18), 6515-6522.

Gerashchenko, S., Sharp, N. S., Neuscamman, S., & Warhaft, Z. (2008). Lagrangian measurements of inertial particle accelerations in a turbulent boundary layer. *Journal of Fluid Mechanics*, *617*, 255-281.

Good, G. H., Ireland, P. J., Bewley, G. P., Bodenschatz, E., Collins, L. R., & Warhaft, Z. (2014). Settling regimes of inertial particles in isotropic turbulence. *Journal of Fluid Mechanics*, *759*, R3.

Hong, J., Toloui, M., Chamorro, L. P., Guala, M., Howard, K., Riley, S., ... & Sotiropoulos, F. (2014). Natural snowfall reveals large-scale flow structures in the wake of a 2.5-MW wind turbine. *Nature communications*, *5*.

Hutchins, N., Chauhan, K., Marusic, I., Monty, J., & Klewicki, J. (2012). Towards reconciling the large-scale structure of turbulent boundary layers in the atmosphere and laboratory. *Boundary-layer meteorology*, *145*(2), 273-306.

Monchaux, R., Bourgoin, M., & Cartellier, A. (2010). Preferential concentration of heavy particles: a Voronoi analysis. *Physics of Fluids (1994-present)*, *22*(10), 103304.

Mordant, N., Crawford, A. M., & Bodenschatz, E. (2004). Experimental Lagrangian acceleration probability density function measurement. *Physica D: Nonlinear Phenomena*, *193*(1), 245-251.

Ouellette, N. T., Xu, H., & Bodenschatz, E. (2006). A quantitative study of three-dimensional Lagrangian particle tracking algorithms. *Experiments in Fluids*, *40*(2), 301-313.

Pruppacher, H. R., & Klett, J. D. (1997). Microphysics of Clouds and Precipitation: With an Introduction to Cloud Chemistry and Cloud Electricity, Springer.

Salazar, J. P., & Collins, L. R. (2012). Inertial particle acceleration statistics in turbulence: Effects of filtering, biased sampling, and flow topology. *Physics of Fluids (1994-present)*, *24*(8), 083302.

Siebert, H., Shaw, R. A., Ditas, J., Schmeissner, T., Malinowski, S. P., Bodenschatz, E., & Xu, H. (2015). High-resolution measurement of cloud microphysics and turbulence at a mountaintop station. *Atmospheric Measurement Techniques*, *8*(8), 3219-3228.

Squires, K. D., & Eaton, J. K. (1991). Preferential concentration of particles by turbulence. *Physics of Fluids A: Fluid Dynamics (1989-1993)*, *3*(5), 1169-1178.

Toloui, M., Riley, S., Hong, J., Howard, K., Chamorro, L. P., Guala, M., & Tucker, J. (2014). Measurement of atmospheric boundary layer based on super-large-scale particle image velocimetry using natural snowfall.*Experiments in Fluids*, *55*(5), 1-14.

Toschi, F., & Bodenschatz, E. (2009). Lagrangian properties of particles in turbulence. *Annual Review of Fluid Mechanics*, *41*, 375-404.

Voth, G. A., la Porta, A., Crawford, A. M., Alexander, J., & Bodenschatz, E. (2002). Measurement of particle accelerations in fully developed turbulence.*Journal of Fluid Mechanics*, *469*, 121-160.

Wang, L. P., & Maxey, M. R. (1993). Settling velocity and concentration distribution of heavy particles in homogeneous isotropic turbulence. *Journal of Fluid Mechanics*, *256*, 27-68.

Wood, A. M., Hwang, W., & Eaton, J. K. (2005). Preferential concentration of particles in homogeneous and isotropic turbulence. *International journal of multiphase flow*, *31*(10), 1220-1230.

Yang, C. Y., & Lei, U. (1998). The role of the turbulent scales in the settling velocity of heavy particles in homogeneous isotropic turbulence. *Journal of Fluid Mechanics*, *371*, 179-205.